Neuro-Oncology
26(5), 826–839, 2024 | https://doi.org/10.1093/neuonc/noad257 | Advance Access date 18 January 2024

Triggering receptor expressed on myeloid cells 2 (TREM2) regulates phagocytosis in glioblastoma

Mekenzie M. Peshoff †, Pravesh Gupta†, Shivangi Oberai, Rakesh Trivedi, Hiroshi Katayama, Prashanth Chakrapani, Minghao Dang, Simona Migliozzi, Joy Gumin, Divya B. Kadri, Jessica K. Lin, Nancy K. Milam, Mark E. Maynard, Brian D. Vaillant, Brittany Parker-Kerrigan, Frederick F. Lang, Jason T. Huse, Antonio Iavarone, Linghua Wang, Karen Clise-Dwyer, and Krishna P. Bhat

All author affiliations are listed at the end of the article

†These authors contributed equally to this work.

Corresponding Authors: Krishna P. Bhat, Department of Translational Molecular Pathology at the University of Texas MD Anderson Cancer Center, Houston, TX, USA (kbhat@mdanderson.org); Pravesh Gupta, Department of Translational Molecular Pathology at the University of Texas MD Anderson Cancer, Houston, TX, USA (pgupta2@mdanderson.org).

Abstract

Background. Glioblastomas (GBMs) are central nervous system tumors that resist standard-of-care interventions and even immune checkpoint blockade. Myeloid cells in the tumor microenvironment can contribute to GBM progression; therefore, emerging immunotherapeutic approaches include reprogramming these cells to achieve desirable antitumor activity. Triggering receptor expressed on myeloid cells 2 (TREM2) is a myeloid signaling regulator that has been implicated in a variety of cancers and neurological diseases with contrasting functions, but its role in GBM immunopathology and progression is still under investigation.

Methods. Our reverse translational investigations leveraged single-cell RNA sequencing and cytometry of human gliomas to characterize TREM2 expression across myeloid subpopulations. Using 2 distinct murine glioma models, we examined the role of Trem2 on tumor progression and immune modulation of myeloid cells. Furthermore, we designed a method of tracking phagocytosis of glioma cells in vivo and employed in vitro assays to mechanistically understand the influence of TREM2 signaling on tumor uptake.

Results. We discovered that TREM2 expression does not correlate with immunosuppressive pathways, but rather showed strong a positive association with the canonical phagocytosis markers lysozyme (LYZ) and macrophage scavenger receptor (CD163) in gliomas. While Trem2 deficiency was found to be dispensable for gliomagenesis, $Trem2^{+}$ myeloid cells display enhanced tumor uptake compared to $Trem2^{-}$ cells. Mechanistically, we demonstrate that TREM2 mediates phagocytosis via Syk signaling.

Conclusions. These results indicate that TREM2 is not associated with immunosuppression in gliomas. Instead, TREM2 is an important regulator of phagocytosis that may be exploited as a potential therapeutic strategy for brain tumors.

Key Points

- TREM2 is not associated with immunosuppressive genes in GBM.
- TREM2 is dispensable for gliomagenesis.
- TREM2 regulates phagocytosis in both human and mouse gliomas.

Importance of the Study

Triggering receptor expressed on myeloid cells 2 (TREM2) has been implicated as a major immunoregulator in both neurological disorders and systemic cancers, yet its functional role in gliomas remains unclear. This study reveals that unlike in other cancers, TREM2 is not associated with immunosuppression in the glioma microenvironment. Instead, TREM2 expression is associated with microglial phagocytosis in both human and mouse gliomas. These findings indicate that TREM2 blockade may not be a viable treatment strategy for gliomas and that the context-dependent complexity of TREM2 signaling in GBM warrants deeper investigations.

Gliomas are the most common primary adult brain tumors and comprise over 80% of central nervous system malignancies.[1] Of these, glioblastomas (GBMs) are high-grade tumors that display the poorest clinical outcome. Despite standard-of-care treatments including surgical resection and concurrent chemoradiation, GBM patients have a median survival of only 15–18 months.[2,3] Although lymphocyte-based immune checkpoint therapies have significantly improved progression-free survival for many other solid tumors, these treatments have yielded disappointing results in clinical trials for GBM.[4,5] Glioma patients are lymphopenic and exhibit T-cell scarcity in the tumor immune microenvironment (TIME), but currently approved immunotherapies continue to target T lymphocytes for facilitating anti-tumor immunity.[6–8]

Recent immunophenotyping studies have revealed that the glioma TIME is characterized by a heterogeneous, predominantly myeloid population.[9–11] These cells include yolk sac-derived, brain resident microglia (MG), bone marrow-derived macrophages (MACs), and monocyte-derived macrophages (MDMs).[11,12] Because of their relative abundance, selective targeting of myeloid cells may be a more viable alternative to current T-cell-based treatments.[13] Myeloid-targeted clinical trials in various cancers are emerging, but a deeper functional understanding of the anti-tumor properties of myeloid cells in GBM is needed.[14] Although MG and MACs perform a variety of protective immunoregulatory functions including phagocytosis of pathogens and cellular debris as well as antigen presentation to T cells, how these pleiotropic functions affect glioma progression remains unclear.[15–17]

Triggering receptor expressed on myeloid cells 2 (TREM2) is a type I transmembrane receptor in the immunoglobulin superfamily that has been implicated as a major regulator of the myeloid cell immune response.[18,19] It is expressed on MACs and MG and is also implicated in dendritic cell (DC) maturation.[18] The binding of its various ligands and association with DNAX activator proteins 10 and 12 (DAP10, DAP12) causes activation of the PI3K-Akt pathway or spleen tyrosine kinase (Syk), resulting in the downstream promotion of cell survival pathways or phagocytosis and cytokine production, respectively.[20] TREM2 is involved in engulfment, a crucial step for the initiation of phagocytosis, and TREM2 deficient or defective MG displays impaired phagocytosis in vitro and in vivo.[21–24] TREM2 is well-characterized in Alzheimer's disease (AD), where the R47H mutation is associated with an increased risk of typical late-onset AD, and TREM2 promotes microglial survival and phagocytosis of amyloid plaques in early-stage AD mouse models.[25–29] Recently, TREM2 has garnered attention for its role in cancer due to its expression on tumor-associated MACs and an increasing interest in the dual role of myeloid cells in the inflammatory response against tumors as well as pro-tumoral immunosuppression.[30,31] Despite the protective role of TREM2 in neurological disorders, its functions in gliomas have been recently reported to be pro-tumorigenic.[32–34]

In this study, we extensively characterize the role of TREM2$^+$ myeloid cells using both human patient-derived glioma tissues as well as orthotopic mouse models. Through comprehensive analysis of a large cohort of human gliomas, we identified a population of glioma-associated TREM2$^+$ myeloid cells that are correlated with phagocytic gene modules. Furthermore, using 2 independent mouse glioma cell lines with different immunogenicity, we demonstrate that although Trem2 is dispensable for glioma control, Trem2$^+$ myeloid cells engulf tumor cells in a Syk-dependent manner. In summary, our investigations ascertain TREM2 as a critical phagocytic immunomodulator in gliomas.

Materials and Methods

Human Brain Tissue Collection

Tissue samples were collected from 56 glioma patients and 5 epilepsy patients. Informed consent and detailed information including age, sex, glioma type, and site of tumor extraction were obtained before neurosurgery. The brain tumor samples were collected according to MD Anderson Internal Review board (IRB)-approved protocols LAB03-0687, LAB04-0001, and 2012-0441, and epileptic brain tissue was collected at Baylor College of Medicine under IRB-approved protocol H-13798. All experiments were performed in compliance with the IRB of UT MD Anderson Cancer Center.

Preparation of Single-Cell Leukocyte Suspensions

Resected brain tumors or tissue from humans and mice were freshly processed or stored overnight in MACS tissue storage solution (Miltenyi Biotech #130-100-008). Tissues were finely minced, and mouse brains were homogenized using a Dounce homogenizer. Tissues were enzymatically dissociated in a warm digestion medium containing 100 µg/ml collagenase D (Sigma–Aldrich #11088866001) and 2 µg/ml DNase for 30 min at 37°C. The reaction was neutralized with 2% fetal bovine serum (FBS) (Gibco #16140-071) in IMDM. Tissues were passed through a 100 µm

cell strainer (Corning #352360) and brain samples were subjected to 33–40% Percoll gradient (Sigma–Aldrich #17-0891-01) to remove myelin, then resuspended in red blood cell (RBC) lysis buffer (Sigma–Aldrich #R7757-100ML) for 10 min at room temperature. The RBC lysis reaction was neutralized with an equal volume of 1X PBS. Cell pellets were obtained via centrifugation at 500g for 5 min at 4°C, and human samples were cryopreserved in 10% DMSO (Sigma–Aldrich #F4135) in FBS in liquid nitrogen at –196° C until use, whereas mouse tissues were collected and processed freshly ahead of experimentation. A detailed description of methods for human leukocyte preparation is provided in our companion manuscript.[11]

Single-Cell RNA,Sequencing, Cytometry, and Computational Analyses

Clinical characteristics, experimental, and computational analyses for sc-RNAseq data generated from glioma-associated CD45$^+$ immune cells of 18 glioma patients are detailed previously.[11] Briefly, expression of TREM2 and phagocytosis pathway gene/s were mapped on myeloid cell types as discussed in this study. Similarly, protein level corroboration for gated TREM2$^+$ and TREM2$^-$ myeloid cell types with MFI of LYZ and CD163 expression was established with 56 glioma patients stratified by IDH and recurrence status. Experimental and corresponding details are elaborated in the Gupta et al. study.[11]

TCGA and GLASS Cohorts

GBMs (528) and 10 nontumor brains from the TCGA dataset analyzed on HG-U133A were used for all GBM correlation analyses (Cancer Genome Atlas Research, 2008). For LGG (grades I and II gliomas), the TCGA dataset containing 513 LGGs was analyzed (https://www.cancer.gov/tcga). Data were visualized and correlation analyses were computed using the GlioVis platform (gliovis.bioinfo.cnio.es), and GEPIA2 was used to visualize survival curves (http://gepia2.cancer-pku.cn).[35] Immunohistochemistry (IHC) was performed on gliomas from the GLASS (Glioma Longitudinal AnalySiS) consortium (glass-consortium.org).[36]

Immunohistochemistry (IHC) and Immunofluorescence (IF)

Formalin-fixed paraffin embedded (FFPE) tissues from human patients and mice were serially sectioned on a microtome at 5 μM. Slides were baked for 30 min at 60 °C then deparaffinized by subsequent washes in xylene, 1:1 xylene, and 100% ethanol, 100% ethanol, 95% ethanol, 70% ethanol, 50% ethanol, and water. Antigen retrieval was performed using a pressure cooker at 100° C for 10 min in sodium citrate pH = 6 buffer. For IHC, slides were washed 3 times in 1X PBS and endogenous peroxidases were blocked with 3% hydrogen peroxide for 30 min. After three washes in PBS, slides were incubated for an hour at room temperature with 10% bovine serum albumin (Millipore Sigma #A7030) to block nonspecific binding. For IF, autofluorescence was blocked with True Black (Biotum #23007) for 5 min followed by 3 washes in deionized water, then background fluorescence was blocked using Background Buster and Fc receptor block (Innovex Biosciences #NB306 and #NB309). Slides were incubated overnight with primary antibody for both IHC and IF (1:100 TREM2 (D8I4C) rabbit mAb, Cell Signaling Technology #91086; 1:1000 Ki-67 (SP6) rabbit mAb, Thermo Fisher #MA5-14520; 1:1000 IBA1 (Ch311H9) chicken mAb, Synaptic Systems #234-009) at 4°C or at room temperature, respectively. After three washes in PBS (IHC) or deionized water (IF), the slides were incubated with the corresponding HRP-conjugated or fluorescent secondary antibody for 1 h at room temperature (goat anti-rabbit IgG (H&L) HRP, Abcam #ab6721; goat anti-rabbit IgG (H&L) Alexa Fluor 488, Invitrogen #A11042; goat anti-chicken IgY Alexa Fluor 594, Invitrogen #A32731). For IHC, slides were washed in PBS 3 times and then developed using a 3,3′-diaminobenzidine (DAB) substrate kit (Abcam #ab64238), then slides were covered in hematoxylin for 3 min and counterstained in PBS for 5–10 min. The slides were dehydrated and coverslipped using an aqueous mounting medium. IHC was assessed using the Olympus BX43 microscope and cellSens software, and IF was imaged with the Keyence BZ-X810 and BZ-X800 viewer. Quantitative analyses were performed blinded using the ImageJ IHC toolkit by multiple authors.

Gene Module Correlation Analyses

For the correlation of phagocytic gene modules to the TREM2 pathway, we included "*TREM2*," "*HCST*," "*TYROBP*," "*APOE*," "*CLU*," "*CD33*," "*LGALS1*," "*LGALS3*," "*GRN*," "*NFATC1*," "*MS4A4A*," "*MS4A6A*." Phagocytic genes were curated from related gene ontology terms containing "Phagocytosis" and the expression values are enlisted in Supplementary Table S1. TREM2 pathway score and phagocytic scores were calculated for each myeloid cell using the Seurat function AddModuleScore.[37] Single-cell RNA-seq data were downloaded from the Brain Immune Atlas database.[38] Phagocytosis-related pathways from MSigDB c5.bp, c5.mf, c5.cc, Hallmark, and KEGG collections of gene sets were used to compute the enrichment in each single myeloid cell using single-sample MWW-GST (ssMWW-GST).[39–41] Pearson's correlation has been used to evaluate the correlation between the gene expression of TREM2 and phagocytosis-related pathways.

Animals

Wildtype C57BL/6J (Jax #000664) and C57BL/6J-Trem2^{em2Adiuj}/J (Jax #027197) mice were procured from the Jackson Laboratory and housed at MD Anderson Department of Veterinary Medicine and Surgery under IACUC-approved protocol #00001504-RN02. Mice used for experiments were sex and age matched.

Murine Cell Lines and In Vivo Glioma Models

For survival studies, 6-month-old mice were intracranially bolted at 2.5 mm lateral and 1 mm anterior to the bregma

according to the guide-screw procedure.[42] One week following bolting, mice were implanted via stereotaxic injection with 2×10^4 CT-2A-luc, 2.0×10^4 CT-2A, or 1.0×10^5 GL261-luc cells resuspended in serum-free DMEM. For flow cytometry analysis, mice were implanted with 5.0×10^4 CT-2A-ZsGreen (CT-2A-ZsG) cells and sacrificed 21 days postinjection. For flank models of glioma, mice were injected subcutaneously in the hind flank with 2.5×10^6 CT-2A cells. Mice in all survival studies were monitored daily for signs of distress and were sacrificed when moribund, as defined by hunched posture, ataxia, and neurological sequelae including seizures. To monitor tumor growth via bioluminescence, mice were injected subcutaneously with 20 µl/g and 15 mg/ml sterile D-luciferin and were imaged using the Perkin-Elmer in vivo imaging system (IVIS 200) 15 min postinjection. Data were analyzed using Aura (Spectral Instruments Imaging) software. CT-2A cells were a gift from Dr. Sourav Ghosh (Yale University) and fingerprinted before use. CT-2A-luc cells were purchased from Sigma–Aldrich (#SCC195) and expanded in-house. CT-2A-ZsG cells were generated using lentiviral particles derived from a pLVX-ZsGreen1C1 vector (Takara Bio #632566). CT-2A and CT-2A-luc were grown in DMEM high glucose with 10% FBS (Gibco #16140-071) and CT-2A-ZsG cells were grown on a puromycin (Thermo Fisher #A1113803) selection cassette at 1 µg/ml. GL-261 cells were grown in DMEM/F12 (Sigma–Aldrich #D8900) containing 10% FBS (Gibco #16140-071). Cells were passaged twice a week or when 70–-80% confluent. Culture medium was aspirated and flasks were washed with sterile 1X PBS, then cells were dissociated through trypsinization (Gibco #T3924100) for 3 min at 37 °C, followed by neutralization with an equal volume of culture medium. Cells were pelleted via centrifugation for 3 min at 400g, then resuspended in culture medium and split 2:1. All cells for experiments were used within the first 5 passages after thawing.

RNA Isolation and NanoString Analysis

Punch biopsy needles (1.5 mm) were used to extract tissue from the tumor core of FFPE mouse brains (Integra #33-31A). The QIAGEN RNeasy FFPE kit (QIAGEN #73504) was used to isolate RNA following deparaffinization. The RNA was sent for nanoString nCounter analysis using the mouse neuroinflammation panel. Statistical analysis of gene expression was performed according to nanoString protocol in the nSolver advanced analysis system and in R.

Flow Cytometry and Staining

Cells were washed twice with 1X PBS then stained with Live Dead Blue Dead dye (Invitrogen #L34962) for 15 min at 4°C. Cells were washed 3 times with FACS buffer (2% FBS in 1X PBS) and then stained for 15 min at 4 °C in Fc block cocktail (1:20 Nova block, Phitonex, Mouse TruStain FcX, Biolegend #101320, CellBlox monocyte/MAC blocking buffer, Invitrogen #B001T07F01). Cells were washed with FACS buffer after staining with Fc block. Cells were stained in an antibody cocktail containing the appropriately titrated antibodies described in Supplementary Table 3 for 20 min at 4 °C. Cells were washed in FACS buffer 3 times and fixed overnight in 200 µl. True Nuclear fixation buffer (Biolegend #73158, #71360) at 4 °C. Data were acquired using the BD LSR Fortessa and Cytek Aurora 5 spectral flow cytometer. Data were analyzed using Cytek SpectroFlo and Becton Dickinson FlowJo 10.8.1.

Sorting of Trem2$^+$ZsG$^+$ Cells

The murine leukocytes (protocol mentioned in preparation of single-cell leukocyte suspension Section of Methods) were stained with CD45, CD11b, and TREM2 (staining protocol mentioned in flow cytometry and staining section of Methods). Sytox Blue (Invitrogen #S34857) was used for the viability determination of cells. Trem2$^+$ZsG$^+$ cells were sorted using BD Influx Silver FACS sorter. The gating strategy is represented in Figure 4.

Cytospin

The Trem2$^+$ZsG$^+$ sorted cells were pooled from a set of 6 mice. The cells were concentrated on Superfrost Adhesion Ringed Cytology slides (Fisher Scientific #22037241) by loading the cells into an EZ Single Cytofunnel (Epredia #A78710003) following manufacturer instructions and centrifuged at 1000 rpm for 4 min.

Western Blotting

Total cell protein was extracted by RIPA buffer containing protease inhibitor and phosphatase inhibitor (TargetMol #C0045). Protein was quantified and separated by SDS–PAGE. Primary antibodies were diluted and incubated overnight at 4 °C. The membranes were then washed with TBST and incubated with HRP-conjugated secondary antibodies (1:3000 dilution) (GenDepot #SA002-500) at room temperature for 1 h. Enhanced chemiluminescence (GenDepot) was performed. The following primary antibodies were purchased from Cell Signaling Technology; TREM2 (# 91068, 1:500 dilution), Syk (# 13198, 1:1000 dilution), mTOR (#2983, 1:1000 dilution), phospho-mTOR Ser 2448 (#2971, 1:1000 dilution), p70 S6 kinase (#2708, 1:1000 dilution), phospho-p70 S6 kinase Thr389 (#9234, 1:1000 dilution). Anti-phospo-Syk antibody was purchased from Novus Biologicals (#MAB6459, 1:1000 dilution). Anti-b-actin antibody was purchased from Millipore Sigma (#A5441, 1:10,000 dilution). For cells subjected to inflammatory conditions, a cytokine cocktail consisting of 5 ng/ml IL-1α (Novus Biologicals #200-LA-002), IL-1β (R&D Systems #201-LB-005/CF), IL-6 (R&D Systems #7270-IL-025/CF), TNF-α (R&D Systems #10291-TA-100), and IFN-γ (R&D Systems #285-IF-100/CF) each was added to cells overnight before harvesting for protein extraction.

In vitro Phagocytosis Assays

HMC3 cells were obtained from ATCC (#CRL-3304) and maintained in EMEM with 10% FBS (Gibco #16140-071). Lentiviral particles were generated from pLV[Exp]-EGFP:T2A:Puro-EF1A > hTREM2 (Vector Builder #VB900014-4782faa) and pLV[Exp]-Puro-EF1A > EGFP (Vector Builder #VB10000-9483amc) vectors and used to

infect early passage HMC3. TREM2-overexpressing HMC3 (TREM2-HMC3) and empty vector HMC3 (EV-HMC3) cells were maintained in media containing 5 µg/ml puromycin (InvivoGen #ant-pr-1). For Syk or mTOR inhibition, cells were treated for 2 h with 1 µM R406 (Selleck Chemicals #S1533) or 1 µM rapamycin (Selleck Chemicals #S1039) respectively. To assess in vitro phagocytosis, EV-HMC3 or TREM2-HMC3 cells were incubated for 2 h at 37°C with 10 µg/ml pHrodo *Escherichia Coli* bioparticles (Invitrogen #P35361) in pH = 7.4 PBS. Phagocytosis was assessed via fluorescence microscopy using the Olympus IX81 microscope and cellSens software, and images were processed using ImageJ.

Results and Discussion

Characterization of TREM2 Expression in Glioma-Associated Myeloid Cells

Although the immunoprotective role of TREM2 in neurodegenerative diseases is well-established, its implication in gliomas is only recently emerging.[32–34] Furthermore, how different glioma pathologies may affect TREM2 expression across myeloid cell subpopulations remains unclear. To address this, we systematically investigated TREM2 expression by utilizing our recent resource study comprised of scRNA-seq and cytometry datasets across human gliomas.[11] Overall, *TREM2* was significantly enriched in myeloid cells compared to lymphoid cells across isocitrate dehydrogenase (IDH) classified gliomas (Supplementary Figure 1A). Within myeloid cells, MG, MAC, MDM, and cDC2 showed the highest expression of *TREM2* across all pathologies (Figure 1A). These observations are consistent with previous studies demonstrating TREM2 restriction to myeloid cells and recent studies showing TREM2 expression in glioma-associated MG and MACs.[18,32,33,43] IF co-staining with MG/MAC marker IBA1 further corroborated our genomic observations that TREM2 is tightly correlated with myeloid cells in GBM (Supplementary Figure 1B).[44] Because MG and MAC phenotypes may be altered by chemo-radiation, we evaluated TREM2 in matched treatment naïve versus recurrent gliomas from the Glioma Longitudinal AnalySiS (GLASS) consortium cohort (Supplementary Table 1) using IHC.[36,45,46] We found that the proportion of TREM2$^+$ cells was significantly higher in IDH-wildtype (IDH-wt) than IDH-mutant (IDH-mut) gliomas, but no differences between primary and recurrent tumors were observed (Figure 1B and Supplementary Figure 1C). However, TREM2$^+$ cells in primary tumors displayed a significantly higher proportion of ramified morphology than in recurrent gliomas regardless of IDH mutation status, which is consistent with the existing dogma that chemotherapy and radiation can influence microglial reactivity (Figure 1C and Supplementary Figure 1D).[47] These results suggest that IDH status and treatment may alter the expression or activation of TREM2$^+$ myeloid cells.

Our extended analyses in a larger cohort of TCGA datasets revealed that expression of *TREM2* and its signaling partner TYRO protein tyrosine kinase-binding protein (*TYROBP)* is associated with higher-grade gliomas and predominant in IDH-wt tumors (Supplementary Figure 1E). We also observed that *TREM2* expression correlated with poor survival only in low- grade gliomas (LGGs), but not in GBMs (Figure 1D and Supplementary Figure 1F). Together, our genomic and proteomic analyses indicate that TREM2 is highly expressed in myeloid cell lineages in IDH-wt high-grade gliomas relative to IDH-mut gliomas.

TREM2 Expression Correlates With Microglial Phagocytosis Pathway Genes But Not Immunosuppression

Recent studies have shown that *TREM2* expression correlates with immunosuppressive genes including *arginase 1* (*ARG1), macrophage receptor with collagenous structure (MARCO), mannose receptor C-type 1 (MRC1),* and *integrin subunit alpha 4 (ITGA4)* in peripheral malignancies such as sarcomas, breast, and colorectal cancers.[30,31,48] Trem2 blockade or deficiency in mouse models of systemic cancers led to TIME remodeling, decreased tumor growth, expression of immunostimulatory molecules on MACs, and increased infiltration of T lymphocytes and NK cells, and similar observations were seen in recent glioma studies.[30,33,34] Our analyses of TCGA glioma datasets showed that although TREM2 correlated with canonical pathway genes such as *TYROBP,* no correlation between *TREM2* and immunosuppressive genes was observed in either GBM or LGG (Figure 2A and Supplementary Figure 2A).[19] TREM2 is known to be a phagocytic mediator, positively regulating the microglial ability to recognize and engulf pathogens through activation of canonical phagocytosis genes in associated pathways.[49,50] We therefore examined if the expression of TREM2 pathway genes (referred to as TREM2 score, see Supplemental Table 2) correlates with phagocytosis gene modules. Using a metagene score derived from genes associated with phagosomes, vesiclemediated transport, and lysosomes (see methods and Supplementary Table 2), we observed that *TREM2* expression/scores showed significant positive correlations with the phagocytosis score in myeloid populations in both internal (Supplementary Figure 2B) and external (Supplementary Figure 2C) scRNA-seq datasets.[38,51,52] MG and MAC/MDMs also showed similar positive correlations of phagocytic score with *TREM2* (Figure 2B). Furthermore, *TREM2* expression was correlated with lysozyme (*LYZ*), a marker for active phagocytosis, and the MAC scavenger receptor *CD163* (Figure 2C) only in MG, but not in MAC/MDMs (Supplementary Figure 2D).[53–55]

Next, we corroborated the expression of TREM2 at the protein level in both MG and non-MG myeloid cell populations in gliomas (Figure 2D). Median fluorescence intensity (MFI) of LYZ and CD163 was used to define their distribution in TREM2-stratified myeloid subsets from primary and recurrent IDH-mut and IDH-wt tumors (n = 9-13/glioma subtype). These analyses revealed that across all tumors, TREM2 was associated with higher expression of LYZ in both MG and MAC, whereas CD163 correlation was seen only in MG (Figure 2E and Supplementary Figure 2E). Even in the TCGA GBM transcriptomic datasets, we observed similar positive correlations between *TREM2* and *CD163* or

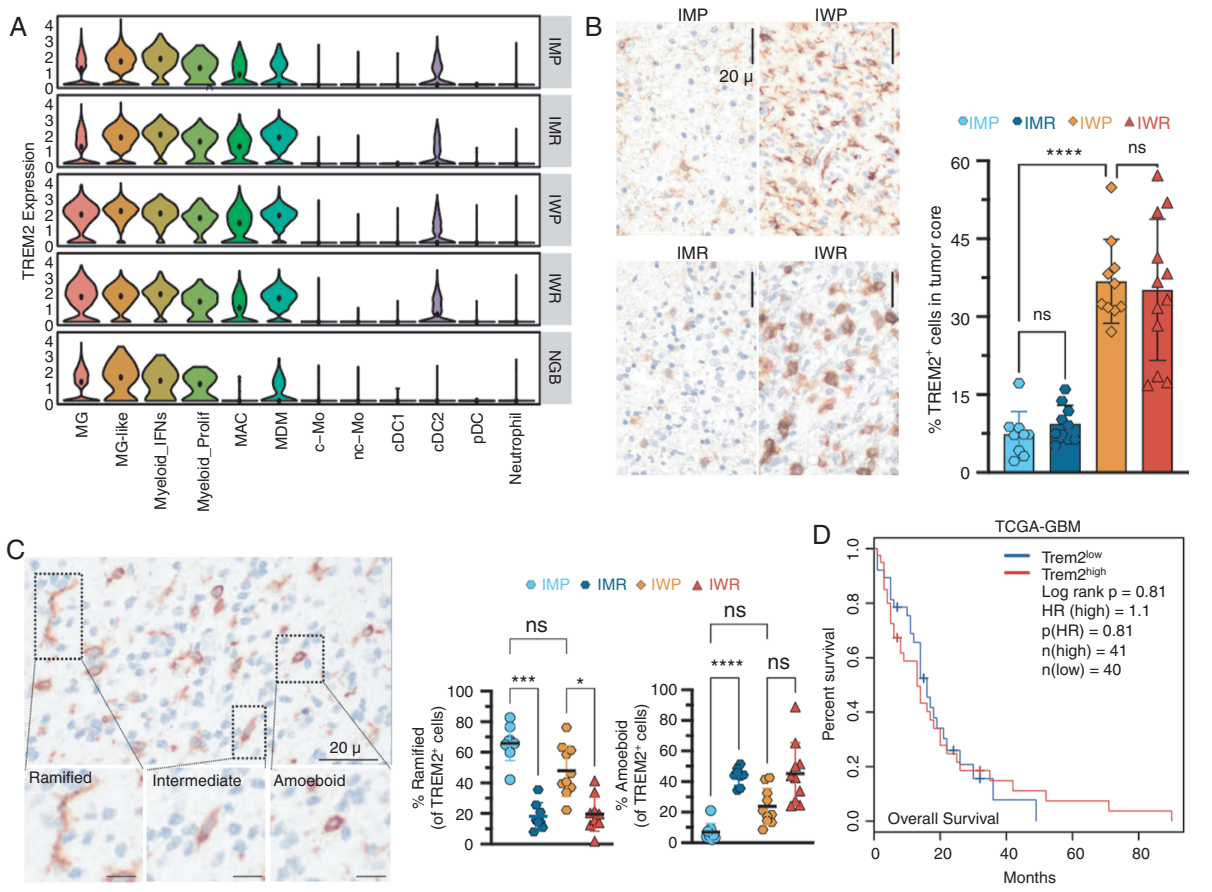

Figure 1. TREM2 is associated with myeloid cells across glioma pathologies and is highly expressed in IDH-wt GBMs. (A) Violin plot showing *TREM2* transcript expression in myeloid cell subsets across human gliomas ($n = 18$) stratified as IMP, IMR, IWP, and IWR and 3 NGB. Clinical characteristics of the patient cohort and myeloid cell types are defined previously.[11] (B-C) Representative IHC staining of TREM2 in human gliomas obtained from GLASS consortium derived FFPE archival tissue as follows: IMP ($n = 9$), IMR ($n = 10$), IWP ($n = 10$), and IWR ($n = 12$), scale bar = 20 µm. (B) TREM2 + cells (left panel) and corresponding bar graphs representing %TREM2+ cells as mean +/– SD in different glioma subtypes (right panel). (C) Magnified areas showing ramified, intermediate, and amoeboid morphology of TREM2+ cells (left panel). Scatter plots representing % of stated morphology of TREM2+ cells as mean ± SD in different glioma subtypes (right panel). In (B and C), each data point represents an average of %TREM2+ cells of three independent tumor regions per patient. Error bars indicate SD of mean. Statistical significance was determined using one-way ANOVA followed by Tukey's multiple comparison test. $^{****}P < 0.0001$, $^{***}P < 0.001$, $^{*}P < 5$, ns = not significant. (D) Kaplan–Meier survival curve showing percent survival of patients stratified by TREM2^{high} (top 25%) and TREM2^{low} (bottom 25%) from TCGA-GBM dataset. Statistical significance was determined using the log-rank test. The number of samples in each group is shown in the inset.

LYZ (Figure 2F). These data demonstrate that TREM2 mRNA and protein correlate with canonical phagocytosis markers in human gliomas.

Trem2 Expression on Myeloid Cells is Dispensable for Glioma Growth

The relevance of MG and MACs in GBM is still evolving due to their remarkable heterogeneity and plasticity, and the lack of appropriate mouse models to distinguish these populations further impedes our understanding.[56] Nevertheless, previous studies have shown a functional distinction of MG and MACs in gliomas. For example, MG regulates phagocytosis even in the absence of MACs, whereas depletion of MACs restrains tumor progression.[9,57,58] However, a recent study claims that depletion of tumor-associated MACs does not improve survival in a murine model of glioma, suggesting context-dependent roles consistent with the clinically heterogeneous presentation of GBM.[56] Given our observations that TREM2 is expressed in myeloid cells across human gliomas, we sought to examine the effect of global *Trem2* deletion on brain tumor growth in syngeneic mouse models (Supplementary Figure 3A). We implanted wildtype (WT) and *Trem2*$^{-/-}$ C57BL/6J mice with GL261-luciferase (GL261-luc) due to its ubiquitous use in preclinical murine studies.[59] When compared to WT mice, *Trem2*$^{-/-}$ glioma-bearing mice showed no significant differences in survival (Figure 3A), which is in contrast to previous studies where *Trem2* deletion caused reduced tumor progression in sarcoma and triple-negative breast cancer models.[30,60] Although the survival differences were not statistically significant, *Trem2*$^{-/-}$ mice showed significantly increased tumor burden compared to WT mice at 15 days after GL261

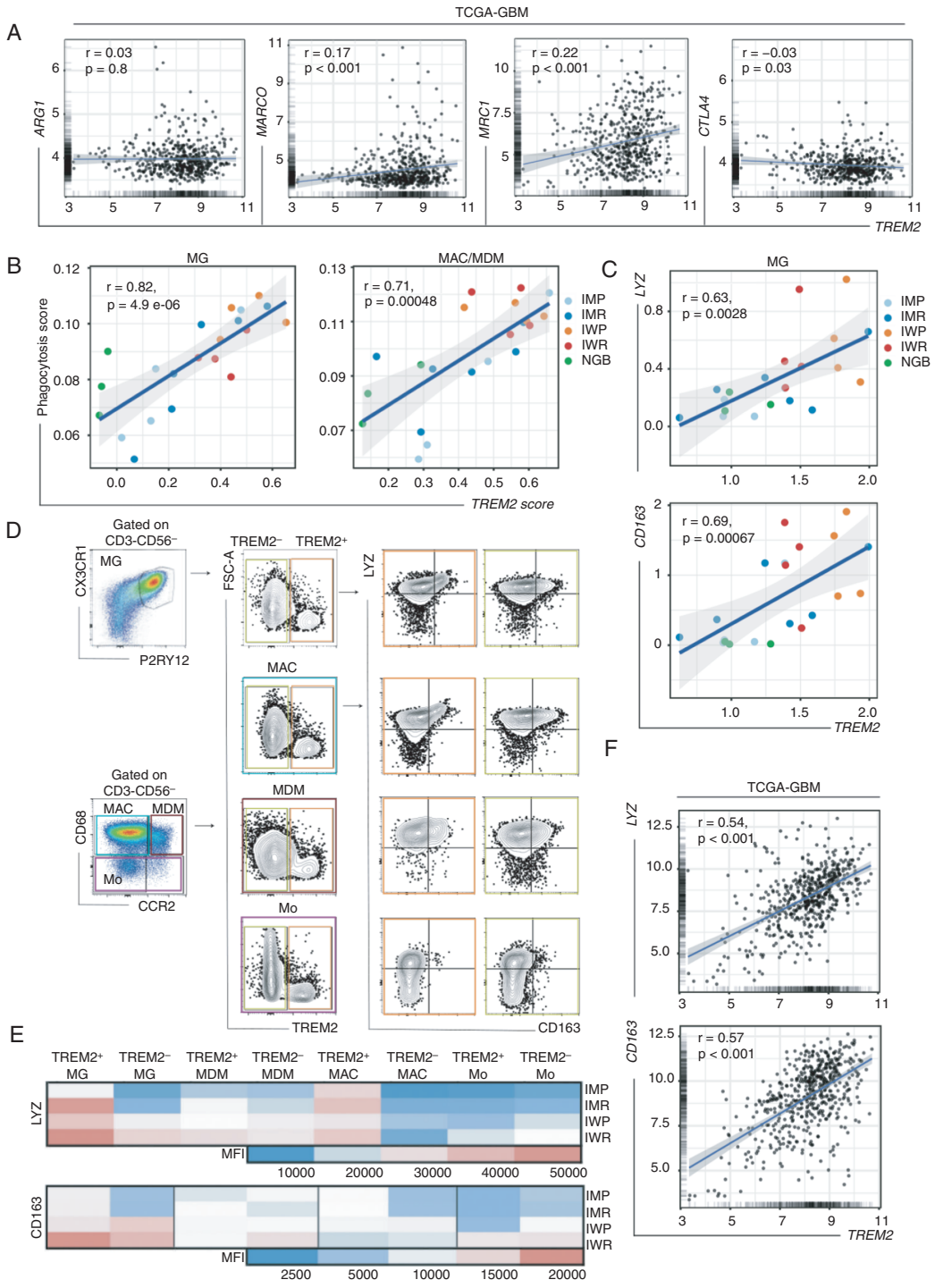

Figure 2. TREM2 is associated with phagocytosis but not immunosuppression in gliomas. (A) Linear regression plots (with corresponding *r* and p-values) showing correlation between *TREM2* (x axis) and indicated immunosuppressive genes (y axis) from TCGA-GBM HG-U133A. *r* value was computed using Pearson's product-moment correlation. Plots were generated using the GlioVis portal.[35] (B and C) Scatter plots (with corresponding *r* and *P*-values) showing the Spearman correlation of (B) mean scores of TREM2 versus phagocytosis pathway genes across glioma patients in MG (left) and MAC/MDM (right) or (C) mean gene expression of *TREM2* versus *LYZ* (top) and *TREM2* vs *CD163* expression (bottom) in MG across glioma patients derived from our sc-RNAseq dataset (Gupta et al., 2022). The blue line in the plot represents the best fit linear regression line, while the gray shadow denotes the confidence interval (95%). Dots are colored by their pathology group. (D) Representative flow cytometry plots showing gating strategy for expression of LYZ and CD163 on TREM2$^+$ and TREM2$^-$ myeloid cell types defined as MG (P2RY12 + CX3CR1 + gated on CD3$^-$CD56$^-$), MAC (CD68$^+$ CCR2$^-$), MDM (CD68$^+$ CCR2$^+$), and Mo (CD68$^-$ CCR2$^+$ gated on CD3$^-$CD56$^-$). (E) Heatmap showing MFI of LYZ and CD163 in TREM2$^+$ vs TREM2$^-$ myeloid cell types (MG, MAC, MDM, Mo). Data was derived from cytometry evaluations the Gupta et al. 2022. (F) Linear regression plots (with corresponding *r* and *P*-values) showing a correlation between *TREM2* vs *LYZ* and *TREM2* vs *CD163* in TCGA-GBM HG-U133A datasets.

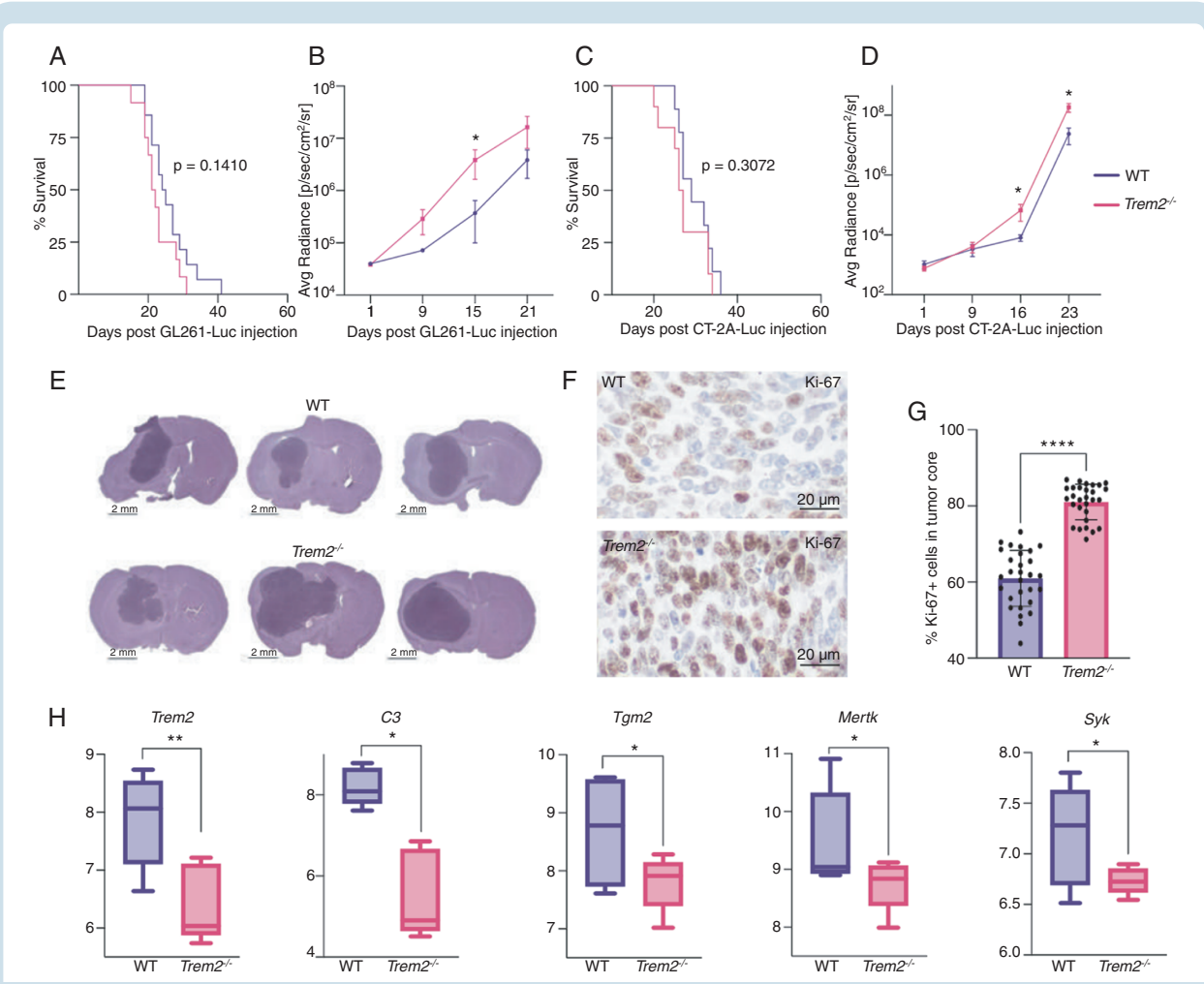

Figure 3. TREM2 deletion does not improve survival in mouse models of glioma. (A) KaplanMeier curve showing % survival in glioma (GL261-luc) bearing WT (purple; $n = 14$) and *Trem2*-/- (pink; $n = 12$) mice. Statistical significance was determined using the Log-rank test at indicated P value. (B) Quantification of bioluminescence in WT and *Trem2*-/- mice bearing GL261-luc at day 1, 9, 15, 21 -tumor implantation. Each point represents average radiance (p/sec/cm^2/sr) values as (log) +/– SD. Statistical significance was determined using Mann–Whitney U test at $^*P < 0.05$. (C) KaplanMeier curve showing % survival in glioma (CT-2A-luc) bearing WT –(purple; $n = 9$) and *Trem2*-/- (pink; $n = 10$) mice. Statistical significance was determined using Log-rank test at the indicated P value. (D) Quantification of bioluminescence in WT and *Trem2*-/- mice bearing CT-2A-luc at day 1, 9, 16, 23 post-tumor implantation. Each point represents average radiance (p/sec/cm^2/sr) values as (log) ± SD. Statistical significance was determined using Mann–Whitney U test at $^*P < 0.05$. (E) H&E staining of glioma bearing brains of WT vs *Trem2*–/– 21 days after CT-2A implantation. Scale bar = 2 mm. (F and G) Representative IHC staining of Ki-67 in the tumor core of CT-2A bearing WT vs *Trem2*–/– mice (Scale bar = 20 µm) is shown in (F) and corresponding bar graphs depicting %Ki-67$^+$ cells as mean ± SD is shown in (G) 21 days after tumor implantation. Error bars indicate SD of the mean. Statistical significance was determined using a Mann–Whitney U test at $^{****}P < 0.0001$. Data are presented from 29 tumor core regions from five mice per group, which were assessed blinded by two experimentalists, and pooled. (H) Boxplots showing the distribution of normalized $\log_2$ transformed counts from nanoString nCounter data of *Trem2*, *C3*, *Tgm2*, *Mertk*, and *Syk* genes between WT and *Trem2*–/– mice ($n = 5$ mice per group). Statistical significance was determined by an independent two sample t-test at $^{**}P < 0.01$, $^*P < 0.05$.

implantation (Figure 3B). Previous studies have shown that murine glioma models show differences in immune response that can be further altered by luciferase transduction.[61,62] To rule out luciferase or cell line-dependent effects, we used another syngeneic mouse glioma cell line with (CT-2A-luc) and without (CT-2A) luciferase to assess the impact of *Trem2* depletion on glioma growth. CT-2A was also chosen due to its appropriateness for immunotherapy studies, relatively low immunogenicity, and histological features reminiscent of human GBM.[63,64] Consistent with the trend observed with GL261-luc, the *Trem2*$^{-/-}$ mice implanted with CT-2A or CT-2A-luc showed no significant differences in survival compared to WT mice (Figure 3C and Supplementary Figure 3B), and gross histological examination of the tumors did not reveal differences in grade or morphology (Figure 3E). However, the kinetics of the tumor growth were significantly higher in *Trem2*$^{-/-}$ mice (Figure 3D and Supplementary Figure 3C), and *Trem2*$^{-/-}$ tumors display an increased proportion of Ki-67$^+$ cells, indicative of enhanced proliferation

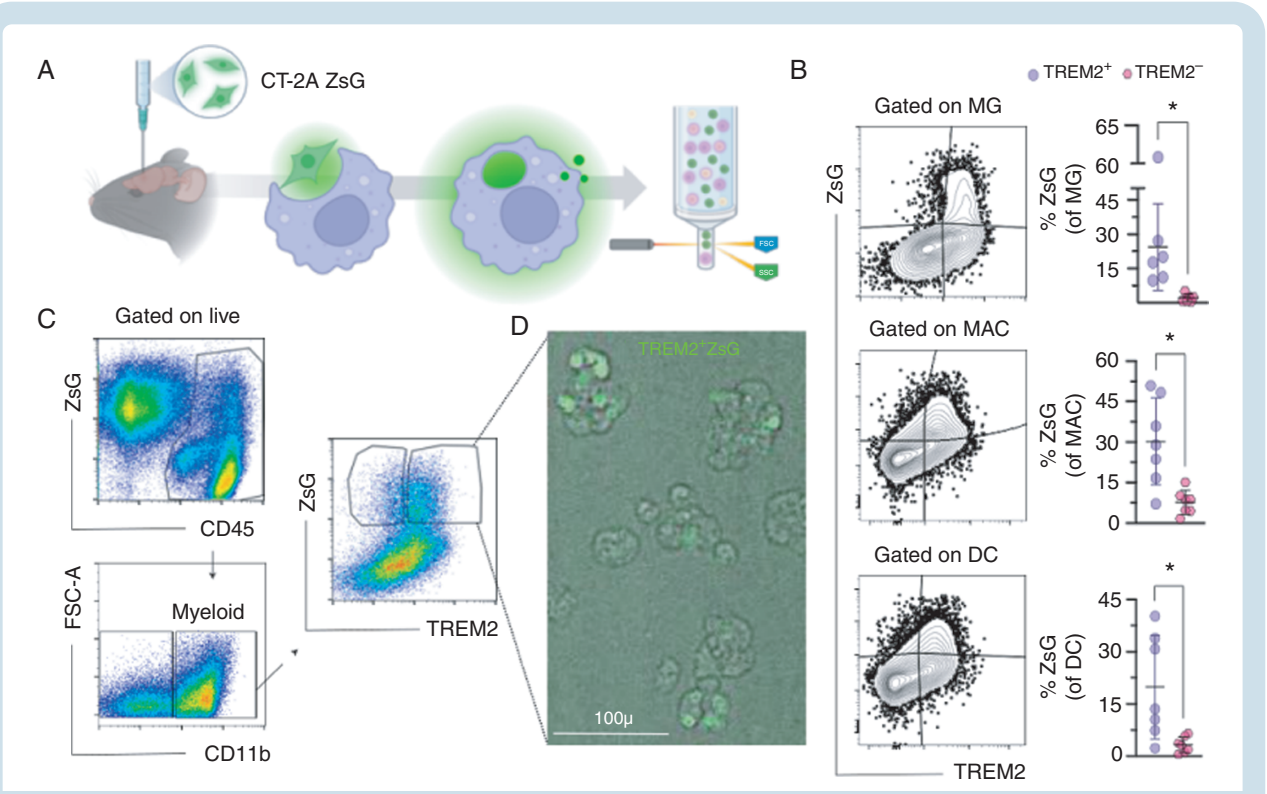

Figure 4. Trem2⁺ myeloid cells exhibit enhanced tumor uptake capacity. (A) Illustration outlining the experimental design of CT-2A-ZsG implantation, phagocytic tumor uptake by myeloid cells, and fluorescence detection via flow cytometry. Schematic created using BioRender. (B) The flow cytometry contour plots show proportions of Trem2 and ZsG on MG, MAC and DC (left), and corresponding scatter plots showing proportions as mean +/– SD of % ZsG tumor uptake by Trem2⁺ and Trem2⁻ of the indicated cell types from glioma bearing WT mice 22 days post-tumor implantation. Error bars indicate the SD of mean. Statistical significance was determined using the Wilcoxon signed-rank test at $*P<0.05$. (C and D) Representative flow cytometry pseudocolor plots depicting a sequential gating of CD45 vs ZsG (gated on live cells), CD11b vs FSC-A (gated on CD45⁺ cells) and Trem2 vs ZsG (gated on CD11b⁺ cells) in (C) and corresponding representative microscopic IF image (scale bar = 100 µm) of flow-sorted Trem2⁺ZsGreen⁺ cells (concentrated by cytospin) as shown in (D) from glioma bearing WT mice post 22 days post-tumor implantation.

compared to WT mice (Figure 3F and 3G). Interestingly, when CT-2A cells were injected subcutaneously into the flanks of mice, the *Trem2*$^{-/-}$ group displayed remarkably reduced tumor volume compared to WT (Supplementary Figure 3D and 3E). Collectively, these data suggest that Trem2 is dispensable for tumor growth in the brain and may in a tumor-suppressive role in gliomas compared to peripheral cancers. Furthermore, our contrasting results in a flank model of glioma raise the possibility of differential roles of Trem2⁺ myeloid cells in the brain compared to peripheral MACs/DCs.

To understand how Trem2 deficiency affects neuroinflammatory pathways in the murine TIME, CT-2A tumors from WT and *Trem2*$^{-/-}$ brains were analyzed using nanoString nCounter to measure changes in ~700 genes involved in neuroinflammation. Comparative differential gene expression (DEG) and gene ontology (GO) analyses revealed significant downregulation of gene families that play a role in the adaptive immune response (eg. *Syk, Btk, Vav1*), inflammation (eg. *Irf8, Msr1*), and MG functions in the *Trem2*$^{-/-}$ group compared to WT mice (Supplementary Figure 3F and 3G). Previous studies have implicated TREM2 as an anti-inflammatory modulator and an important regulator of MG survival, so it is not surprising that these functions were reduced in the TIME of *Trem2*$^{-/-}$ mice.[65,66] However, several genes in the MG autophagic pathway (eg. *Mertk, Tgm2*) were downregulated in *Trem2*$^{-/-}$ mice (Figure 3H). It is noteworthy that previous studies have linked autophagic machinery to microglial phagocytosis, and TREM2 may function through these pathways to regulate glioma growth.[67,68]

Trem2⁺ Myeloid Cells Mediate Phagocytosis of Gliomas

To further investigate the functional role of Trem2⁺ myeloid cells in mouse gliomas, we generated CT-2A-ZsGreen (CT-2A-ZsG), a reporter cell line to visualize the uptake of tumor-derived fluorescent protein by myeloid cells. As ZsG-expressing cancer cells are phagocytosed, the fluorescence can be detected by flow cytometry, making CT-2A-ZsG a useful model for tracking phagocytosis and tumor uptake (Figure 4A).[69] We implanted CT-2A-ZsG cells directly into the caudate nucleus of WT C57BL/6 mice, and 21 days after implantation, mice were sacrificed and their brains were analyzed via flow cytometry, allowing for the interrogation of Trem2⁺ZsG⁺ cells in MG, MAC, and DCs. ZsG was detected in the

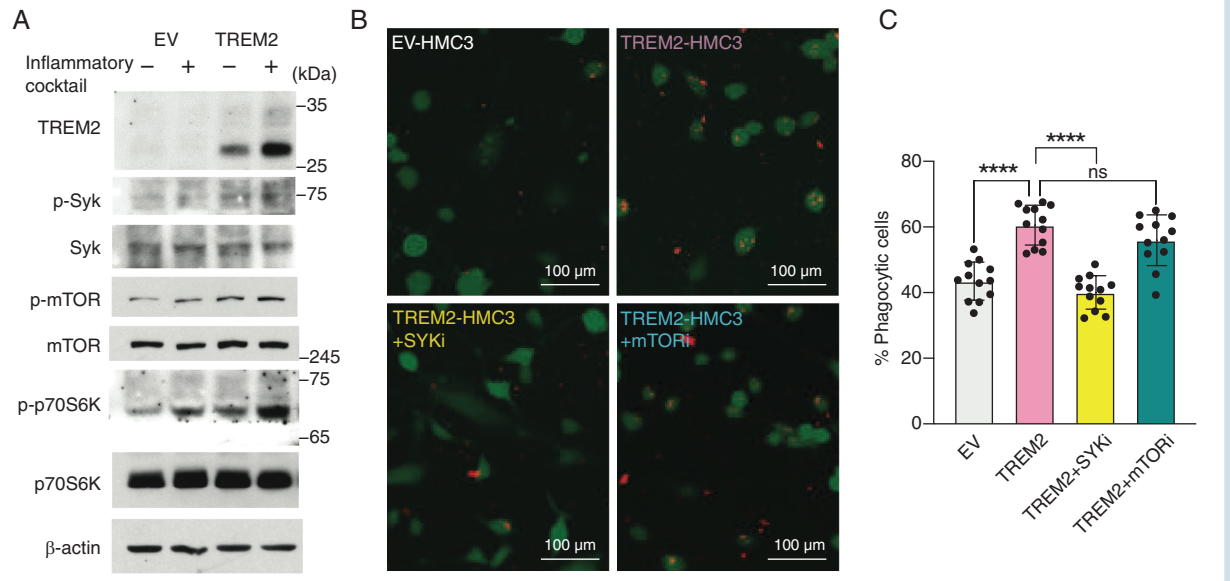

Figure 5. TREM2 mediates phagocytosis via the Syk pathway. (A) Western blot showing expression of TREM2, Syk, p-Syk, mTOR, p-mTOR, p70S6K, and p-p70S6K in EV or TREM2-overexpressing HMC3 cells. For inflammatory groups, cells were incubated overnight with a cytokine cocktail (IL-1α, IL-1β, IL-6, TNF-α, IFN-γ, 5 ng/ml each). (B) Representative IF images of pHrodo particles (red) within HMC3 transduced with empty vector (EV-HMC3) or TREM2 (TREM2-HMC3) are shown (top panel). The lentiviral vectors used for transduction express GFP. Representative IF images of pHrodo incubation with TREM2-HMC3 treated with either Syk inhibitor or mTOR inhibitor for 2 h before phagocytosis assay (bottom panel). Scale bar = 100 µm. (C) Bar graph representing proportions of % phagocytosis as mean ± SD of EV-HMC3, TREM2-HMC3, TREM2-HMC3 with Syk inhibitor, and TREM2-HMC3 with mTOR inhibitor. Triplicates from 4 independent experiments were pooled for analysis and error bars represent the SD of the mean. Statistical significance was determined by one-way ANOVA; **** $P < 0.0001$, ns = not significant.

brains of the glioma-bearing mice, specifically in myeloid subsets, confirming its efficacy as a phagocytosis surrogate. In line with our human studies, we observed the expression of Trem2 on MG, MACs, and DCs (Figure 4B). Across these myeloid subpopulations, we found that Trem2$^+$ cells showed significantly higher phagocytic uptake of ZsG$^+$ tumor cells when compared to Trem2$^-$ cells (Figure 4B and Supplementary Figure 4A and B). To rule out Trem2$^+$ZsG$^+$ cells as technical doublets, we sorted these cells and confirmed by cytospin that CT-2A-ZsG tumor cells were indeed phagocytosed by Trem2$^+$ myeloid cells (Figure 4C and D). These in vivo results implicate Trem2 as a key phagocytic regulator in gliomas.

TREM2 Regulates Phagocytosis via the Syk Pathway

Previous studies have shown that TREM2 dependent phagocytosis requires activation of Syk, a central regulator of signal transduction downstream of TREM2, and that deletion of Syk impairs microglial activation.[70–72] To mechanistically examine the involvement of this pathway in TREM2-mediated phagocytosis, we overexpressed TREM2 in the human microglial cell line HMC3.[73] As shown previously, TREM2 was undetectable in this line under basal conditions (Figure 5A).[74] We overexpressed TREM2 in these cells using lentiviral transduction and examined the levels of key proteins downstream of TREM2 signaling. Overexpression of TREM2 increased p-Syk, p-mTOR, and p-p70S6K levels, and correspondingly increased phagocytosis as determined by engulfment of *E. coli* conjugated to a pH-sensitive fluorogenic dye (pHrodo, Figure 5A-C). Because TREM2 expression has been shown to modulate levels of inflammatory cytokines including IL-1β and IL-6, we investigated if incubation with an inflammatory cytokine cocktail could affect TREM2 expression and phosphorylation of its downstream targets.[75] Overnight incubation with a 5 ng/ml cocktail of inflammatory cytokines (IL-1α, IL-1β, IL-6, TNF-α, and IFN-γ), resulted in an increase in Syk, mTOR, and p70S6K phosphorylation (Figure 5A) but did not significantly affect phagocytosis (data not shown). Because Syk deficiency ultimately inhibits mTOR signaling via PI3K/Akt, we wanted to determine if the enhanced phagocytosis in TREM2-HMC3 was dependent on Syk itself or its downstream pathways.[72] Pharmacological inhibition of Syk, but not mTOR, blocked TREM2-driven induction of phagocytosis (Figure 5B and C), implying a crucial role for Syk signaling in this process.

Collectively, our reverse translational evaluations with glioma patients and in vivo mouse models position TREM2 as an important regulator of phagocytosis in GBM. Emerging studies show both cell intrinsic as well immunomodulatory roles of TREM2 in cancer.[76] TREM2 can function as either an oncogene or tumor suppressor in cancer cells, but most studies have highlighted immunosuppressive functions of TREM2 given its high expression in tumor-associated MACs.[19,30,31] Other studies have suggested that TREM2 may have an oncogenic function in gliomas.[32–34] However, our investigation reveals

that the role of TREM2 in brain tumors is likely complex and highly context-dependent.[33,34] For example, mouse models of glioma vary widely in their backgrounds and immunogenicity.[77] Our studies utilize cell lines created by methylcholanthene injection into the brain (CT-2A and GL261), whereas the SB28 line, which was used in a recent study with contrasting results from ours, was generated via sleeping beauty transposon.[33] GL261 is highly immunogenic and expresses MHC class I and despite its lower immunogenicity, CT-2A also displays moderate expression of MHC class I.[63] In contrast to these lines, SB28 is remarkably low in MHC class I, leading to distinct responses to immune checkpoint blockade in mouse glioma models.[59,78] With the recent discovery of MHC class I-independent NK cell killing mechanisms in GBM, it is possible that differential MHC class I expression in mouse glioma lines activates distinct anti-tumor immune pathways.[79] Even in the same cell line, sex, and age can impact TREM2 dynamics.[34,80] Therefore, additional validation should be performed using male and female mice across the lifespan to better understand how these variables impact Trem2 expression and survival in glioma models. Additionally, all reported studies on TREM2's role in glioma employ global *Trem2*$^{-/-}$ animals, which do not allow for interrogation of cell type specific effects mediated by Trem2^{+} MG, infiltrating MACs, or other transient myeloid cells, which is warranted given the contrasting results of glioma growth in the brain versus flanks of *Trem2*$^{-/-}$ mice. Although beyond the scope of this study, our future directions include developing conditional Trem2 knockout mouse models. This would enable the investigation of differential functions of Trem2^{+} MG or MACs in gliomas. Because previous studies have shown a reduced number of MG in *Trem2*$^{-/-}$ mice and myeloid compensatory mechanisms in GBM, conclusions drawn from glioma studies employing *Trem2*$^{-/-}$ mice should be interpreted carefully.[81,82]

Nonetheless, our study suggests that, at least in certain contexts, blocking TREM2 in gliomas may not be a feasible immunotherapeutic strategy as suggested in other cancers or other glioma cell lines.[43] Rather, TREM2 may play a protective role like in AD, wherein loss of TREM2 alters microglial behavior including reduced phagocytosis and amyloid clearance.[83] Therefore, strategies to boost TREM2 function by stabilization and reducing its membrane shedding could be glioma-specific treatment approaches that need to be explored. It is interesting to note that while TREM2 is associated with phagocytosis in the glioma microenvironment, we did not find its expression to be correlated with improved survival in GBM patients. It is possible that although TREM2^{+} phagocytes engulf cancer cells, the kinetics of the tumor's growth and invasion outpace innate immune surveillance. Cancer cells can also evade engulfment by upregulating the "don't eat me" transmembrane protein CD47, but mechanisms of immune escape remain to be explored in this context.[84] Furthermore, this study did not examine the effects of radiation therapy on phagocytosis, and because dead cells are particularly prone to phagocytic uptake, combining TREM2 stabilization with radiation or chemotherapy could help to better understand TREM2's functional role within a clinical context.[85] Despite these limitations, this study reveals a novel protective role of TREM2^{+} myeloid cells in GBM, highlighting the necessity for further investigation into TREM2 in additional GBM models.

Supplementary material

Supplementary material is available online at *Neuro-Oncology* (https://academic.oup.com/neuro-oncology).

Keywords

TREM2 | glioblastoma | phagocytosis | microglia

Funding

This study was supported by the generous philanthropic contributions to The University of Texas (UT) MD Anderson Cancer Center (MDACC) Moon Shots Program. Part of this study was also supported by NIH grants: R21 CA222992 and R01 CA225963 to K.P.B. This study was partly supported by the UT MDACC start-up research fund to L.W. We thank the American Legion Auxiliary Fellowship in Cancer Research supporting M.M.P. We also thank the UT MDACC Odyssey fellowship programs for their generous training fellowship support and the UT MDACC Divisional Research award and CPRIT pilot grant to P.G. We would like to acknowledge Lisa Norberg and Brain Tumor Center Histology Core for assistance with tissue processing, Luisa Solis Soto for assistance with IHC, Chrystine Gallegos for assistance with IF, Advanced Cytometry and Sorting Facility (ACSF), Small Animal Imaging Facility (SAIF) and Advanced Technology Genomics Core (ATGC) core facilities at MD Anderson and the Baylor College of Medicine Gene Vector Core for support with experiments. The ATGC facility is supported by NCI grant 520 CA016672; ACSF is supported by NCI P30 CA016672; SAIF is supported by Cancer Center Support Grant CA16672. Finally, we wish to acknowledge the patients and their families whose generous donations made this study possible. In honor of Barry Lane Johnson (1950-2020).

Author contributions

Conception of the study: KPB and PG; experimental design and implementation: MMP, PG, SO, KPB; data collection, experimentation, and analysis: MMP, PG, SO, RT, HK, MD, SM, JG, DBK, JKL, NKM, MEM, BDV, AI, LW, KCD; collection of tissue and clinical information: BPK, FFL, JTH. MMP, PG, SO, and KPB wrote the manuscript with input from all authors.

Affiliations

Department of Translational Molecular Pathology, Neurosurgery at the University of Texas MD Anderson Cancer Center, Houston,

Texas, USA (M.M.P., P.G., S.O., R.T., H.K., P.C., D.B.K., J.K.L., N.K.M., J.T.H., K.P.B.); Department of Genomic Medicine, Neurosurgery at the University of Texas MD Anderson Cancer Center, Houston, Texas, USA (M.D., L.W.); Department of Hematopoietic Biology & Malignancy, Neurosurgery at the University of Texas MD Anderson Cancer Center, Houston, Texas, USA (K.C.-D.); Department of Translational Molecular Pathology, Neurosurgery at the University of Texas MD Anderson Cancer Center, Houston, Texas, USA (J.G., P.-K., F.F.L., K.P.B.); Department of Translational Molecular Pathology, The University of Texas, MD Anderson Cancer Center, UTHealth Houston Graduate School of Biomedical Sciences, Houston, Texas, USA; (M.M.P., J.T.H., K.P.B.); Department of Electrical and Computer Engineering, University of Houston, Houston, Texas, USA (M.E.M.); Departments of Translational Molecular Pathology, Dell Medical School, University of Texas at Austin, Austin, Texas, USA (B.D.V.); Department of Neurological Surgery, Sylvester Comprehensive Cancer Center at the University of Miami Miller School of Medicine, Miami, Florida, USA (S.M., A.I.)

References

1. Ostrom QT, et al. CBTRUS statistical report: primary brain and central nervous system tumors diagnosed in the United States in 2008–2012. *Neuro Oncol.* 2015;17(Suppl 4):iv1–iv62.
2. Stupp R, Mason WP, van den Bent MJ, et al. European Organisation for Research and Treatment of Cancer Brain Tumor and Radiotherapy Groups. Radiotherapy plus concomitant and adjuvant temozolomide for glioblastoma. *N Engl J Med.* 2005;352(10):987–996.
3. Hegi ME, Diserens A-C, Gorlia T, et al. MGMT gene silencing and benefit from temozolomide in glioblastoma. *N Engl J Med.* 2005;352(10):997–1003.
4. Reardon DA, Brandes AA, Omuro A, et al. Effect of nivolumab vs bevacizumab in patients with recurrent glioblastoma: the checkmate 143 phase 3 randomized clinical trial. *JAMA Oncol.* 2020;6(7):1003–1010.
5. Sade-Feldman M, Yizhak K, Bjorgaard SL, et al. Defining T cell states associated with response to checkpoint immunotherapy in melanoma. *Cell.* 2018;175(4):998–1013.e20.
6. Kim WJ, Dho Y-S, Ock C-Y, et al. Clinical observation of lymphopenia in patients with newly diagnosed glioblastoma. *J Neurooncol.* 2019;143(2):321–328.
7. Klemm F, Maas RR, Bowman RL, et al. Interrogation of the microenvironmental landscape in brain tumors reveals disease-specific alterations of immune cells. *Cell.* 2020;181(7):1643–1660.e17.
8. Friebel E, Kapolou K, Unger S, et al. Single-cell mapping of human brain cancer reveals tumor-specific instruction of tissue-invading leukocytes. *Cell.* 2020;181(7):1626–1642.e20.
9. Chen Z, Feng X, Herting CJ, et al. Cellular and molecular identity of tumor-associated macrophages in glioblastoma. *Cancer Res.* 2017;77(9):2266–2278.
10. Larkin CJ, Arrieta VA, Najem H, et al. Myeloid cell classification and therapeutic opportunities within the glioblastoma tumor microenvironment in the single cell-omics era. *Front Immunol.* 2022;13:907605.
11. Gupta P, Dang M, Oberai S, et al. Immune landscape of isocitrate dehydrogenase stratified human gliomas. *bioRxiv.* 2022:2022.2011.2008.514794.
12. Morantz RA, Wood GW, Foster M, Clark M, Gollahon K. Macrophages in experimental and human brain tumors. Part 1: studies of the macrophage content of experimental rat brain tumors of varying immunogenicity. *J Neurosurg.* 1979;50(3):298–304.
13. Quail DF, Joyce JA. Molecular pathways: deciphering mechanisms of resistance to macrophage-targeted therapies. *Clin Cancer Res.* 2017;23(4):876–884.
14. Cassetta L, Pollard JW. Targeting macrophages: therapeutic approaches in cancer. *Nat Rev Drug Discov.* 2018;17(12):887–904.
15. Barker RN, Erwig L-P, Hill KSK, et al. Antigen presentation by macrophages is enhanced by the uptake of necrotic, but not apoptotic, cells. *Clin Exp Immunol.* 2002;127(2):220–225.
16. Schetters STT, Gomez-Nicola D, Garcia-Vallejo JJ, Van Kooyk Y. Neuroinflammation: Microglia and T cells get ready to Tango. *Front Immunol.* 2017;8:1905.
17. Brown GC, Neher JJ. Microglial phagocytosis of live neurons. *Nat Rev Neurosci.* 2014;15(4):209–216.
18. Bouchon A, Hernandez-Munain C, Cella M, Colonna M. A DAP12-mediated pathway regulates expression of CC chemokine receptor 7 and maturation of human dendritic cells. *J Exp Med.* 2001;194(8):19411111122.
19. Deczkowska A, Weiner A, Amit I. The physiology, pathology, and potential therapeutic applications of the TREM2 signaling pathway. *Cell.* 2020;181(6):1207–1217.
20. Peng Q, Malhotra S, Torchia JA, et al. TREM2- and DAP12-dependent activation of PI3K requires DAP10 and is inhibited by SHIP1. *Sci Signal* 2010;3(122):ra38.
21. Takahashi K, Rochford CD, Neumann H. Clearance of apoptotic neurons without inflammation by microglial triggering receptor expressed on myeloid cells-2. *J Exp Med.* 2005;201(4):647–657.
22. Kleinberger G, Brendel M, Mracsko E, et al. The FTD-like syndrome causing TREM2 T66M mutation impairs microglia function, brain perfusion, and glucose metabolism. *EMBO J.* 2017;36(13):1837–1853.
23. N'Diaye EN, Branda CS, Branda SS, et al. TREM-2 (triggering receptor expressed on myeloid cells 2) is a phagocytic receptor for bacteria. *J Cell Biol.* 2009;184(2):215–223.
24. Ulrich JD, Finn MB, Wang Y, et al. Altered microglial response to Abeta plaques in APPPS1-21 mice heterozygous for TREM2. *Mol Neurodegener.* 2014;9:20.
25. Jonsson T, Stefansson H, Steinberg S, et al. Variant of TREM2 associated with the risk of Alzheimer's disease. *N Engl J Med.* 2013;368(2):107–116.
26. Guerreiro R, Wojtas A, Bras J, et al; Alzheimer Genetic Analysis Group. TREM2 variants in Alzheimer's disease. *N Engl J Med.* 2013;368(2):117–127.
27. Wang Y, Cella M, Mallinson K, et al. TREM2 lipid sensing sustains the microglial response in an Alzheimer's disease model. *Cell.* 2015;160(6):1061–1071.
28. Ulland TK, Song WM, Huang SC, et al. TREM2 maintains microglial metabolic fitness in Alzheimer's disease. *Cell.* 2017;170(4):649–663.e13.
29. Wang Y, Ulland TK, Ulrich JD, et al. TREM2-mediated early microglial response limits diffusion and toxicity of amyloid plaques. *J Exp Med.* 2016;213(5):667–675.
30. Molgora M, Esaulova E, Vermi W, et al. TREM2 modulation remodels the tumor myeloid landscape enhancing anti-PD-1 immunotherapy. *Cell.* 2020;182(4):886–900.e17.
31. Katzenelenbogen Y, Sheban F, Yalin A, et al. Coupled scRNA-Seq and intracellular protein activity reveal an immunosuppressive role of TREM2 in Cancer. *Cell.* 2020;182(4):872–885.e19.
32. Yu M, Chang Y, Zhai Y, et al. TREM2 is associated with tumor immunity and implies poor prognosis in glioma. *Front Immunol.* 2022;13:1089266.
33. Sun R, Han R, McCornack C, et al. TREM2 inhibition triggers antitumor cell activity of myeloid cells in glioblastoma. *Sci Adv.* 2023;9(19):eade3559.
34. Chen X, Zhao Y, Huang Y, et al. TREM2 promotes glioma progression and angiogenesis mediated by microglia/brain macrophages. *Glia.* 2023;71(11):2679–2695.

35. Bowman RL, Wang Q, Carro A, Verhaak RG, Squatrito M. GlioVis data portal for visualization and analysis of brain tumor expression datasets. *Neuro Oncol.* 2017;19(1):139–1141.
36. Consortium G. Glioma through the looking GLASS: molecular evolution of diffuse gliomas and the glioma longitudinal analysis consortium. *Neuro Oncol.* 2018;20(7):873–884.
37. Butler A, Hoffman P, Smibert P, Papalexi E, Satija R. Integrating single-cell transcriptomic data across different conditions, technologies, and species. *Nat Biotechnol.* 2018;36(5):411–420.
38. Pombo Antunes AR, Scheyltjens I, Lodi F, et al. Single-cell profiling of myeloid cells in glioblastoma across species and disease stage reveals macrophage competition and specialization. *Nat Neurosci.* 2021;24(4):595–610.
39. Garofano L, Migliozzi S, Oh YT, et al. Pathway-based classification of glioblastoma uncovers a mitochondrial subtype with therapeutic vulnerabilities. *Nat Cancer.* 2021;2(2):141–156.
40. Frattini V, Pagnotta SM, Tala, et al. A metabolic function of FGFR3-TACC3 gene fusions in cancer. *Nature.* 2018;553(7687):222–227.
41. Migliozzi S, Oh YT, Hasanain M, et al. Integrative multi-omics networks identify PKCdelta and DNA-PK as master kinases of glioblastoma subtypes and guide targeted cancer therapy. *Nat Cancer.* 2023;4(2):181–202.
42. Lal S, Lacroix M, Tofilon P, et al. An implantable guide-screw system for brain tumor studies in small animals. *J Neurosurg.* 2000;92(2):326–333.
43. Qiu H, Shao Z, Wen X, et al. TREM2: keeping pace with immune checkpoint inhibitors in cancer immunotherapy. *Front Immunol.* 2021;12:716710.
44. Sasaki, Y., Ohsawa, K., Kanazawa, H., Kohsaka, S. Imai, Y. Iba1 is an actin-cross-linking protein in macrophages/microglia. *Biochem Biophys Res Commun.* 2001;286:292–297.
45. Wei J, Chen P, Gupta P, et al. Immune biology of glioma-associated macrophages and microglia: functional and therapeutic implications. *Neuro Oncol.* 2020;22(2):180–194.
46. Gabrusiewicz K, Rodriguez B, Wei J, et al. Glioblastoma-infiltrated innate immune cells resemble M0 macrophage phenotype. *JCI Insight.* 2016;1(2):e85841.
47. Nimmerjahn A, Kirchhoff F, Helmchen F. Resting microglial cells are highly dynamic surveillants of brain parenchyma in vivo. *Science.* 2005;308(5726):1314–1318.
48. Khantakova D, Brioschi S, Molgora M. Exploring the impact of TREM2 in tumor-associated macrophages. *Vaccines (Basel).* 2022;10(6):943.
49. Krasemann S, Madore C, Cialic R, et al. The TREM2-APOE pathway drives the transcriptional phenotype of dysfunctional microglia in neurodegenerative diseases. *Immunity.* 2017;47(3):566–581.e9.
50. Yeh FL, Wang Y, Tom I, Gonzalez LC, Sheng M. TREM2 binds to apolipoproteins, including APOE and CLU/APOJ, and thereby facilitates uptake of amyloid-beta by microglia. *Neuron.* 2016;91(2):328–340.
51. Yu K, Hu Y, Wu F, et al. Surveying brain tumor heterogeneity by single-cell RNA-sequencing of multi-sector biopsies. *Natl Sci Rev.* 2020;7(8):1306–1318.
52. Neftel C, Laffy J, Filbin MG, et al. An integrative model of cellular states, plasticity, and genetics for glioblastoma. *Cell.* 2019;178(4):835–849.e21.
53. Venezie RD, Toews AD, Morell P. Macrophage recruitment in different models of nerve injury: lysozyme as a marker for active phagocytosis. *J Neurosci Res.* 1995;40(1):99–107.
54. Schulz D, Severin Y, Zanotelli VRT, Bodenmiller B. In-depth characterization of monocyte-derived macrophages using a mass cytometry-based phagocytosis assay. *Sci Rep.* 2019;9(1):1925.
55. Colton C, Wilcock DM. Assessing activation states in microglia. *CNS Neurol Disord Drug Targets.* 2010;9(2):174–191.
56. Chipman ME, Wang Z, Sun D, et al. Tumor progression is independent of tumor-associated macrophages in cell lineage-based mouse models of glioblastoma. *Proc Natl Acad Sci U S A.* 2023;120(16):e2222084120.
57. Hutter G, Theruvath J, Graef CM, et al. Microglia are effector cells of CD47-SIRPalpha antiphagocytic axis disruption against glioblastoma. *Proc Natl Acad Sci U S A.* 2019;116(3):997–11006.
58. Pyonteck SM, Akkari L, Schuhmacher AJ, et al. CSF-1R inhibition alters macrophage polarization and blocks glioma progression. *Nat Med.* 2013;19(10):1264–1272.
59. Haddad AF, Young JS, Amara D, et al. Mouse models of glioblastoma for the evaluation of novel therapeutic strategies. *Neurooncol Adv.* 2021;3(1):vdab100.
60. Timperi E, Gueguen P, Molgora M, et al. Lipid-associated macrophages are induced by cancer-associated fibroblasts and mediate immune suppression in breast cancer. *Cancer Res.* 2022;82(18):3291–3306.
61. Podetz-Pedersen KM, Vezys V, Somia NV, Russell SJ, McIvor RS. Cellular immune response against firefly luciferase after sleeping beauty-mediated gene transfer in vivo. *Hum Gene Ther.* 2014;25(11):955–965.
62. Sanchez VE, Lynes JP, Walbridge S, et al. GL261 luciferase-expressing cells elicit an anti-tumor immune response: an evaluation of murine glioma models. *Sci Rep.* 2020;10(1):11003.
63. Nakashima H, Alayo QA, Penaloza-MacMaster P, et al. Modeling tumor immunity of mouse glioblastoma by exhausted CD8(+) T cells. *Sci Rep.* 2018;8(1):208.
64. Liu CJ, Schaettler M, Blaha DT, et al. Treatment of an aggressive orthotopic murine glioblastoma model with combination checkpoint blockade and a multivalent neoantigen vaccine. *Neuro Oncol.* 2020;22(9):1276–1288.
65. Turnbull IR, Gilfillan S, Cella M, et al. Cutting edge: TREM-2 attenuates macrophage activation. *J Immunol.* 2006;177(6):3520–3524.
66. Zheng H, Jia L, Liu C-C, et al. TREM2 promotes microglial survival by activating wnt/beta-catenin pathway. *J Neurosci.* 2017;37(7):1772–11784.
67. Berglund R, Guerreiro-Cacais AO, Adzemovic MZ, et al. Microglial autophagy-associated phagocytosis is essential for recovery from neuroinflammation. *Sci Immunol.* 2020;5(52):eabb5077.
68. Li G, Sherchan P, Tang Z, Tang J. Autophagy & phagocytosis in neurological disorders and their possible cross-talk. *Curr Neuropharmacol.* 2021).;19(11):1912–1924.
69. Bowman-Kirigin JA, Desai R, Saunders BT, et al. The conventional dendritic cell 1 subset primes CD8+ T cells and traffics tumor antigen to drive antitumor immunity in the brain. *Cancer Immunol Res.* 2023;11(1):20–37.
70. Hall-Roberts H, Agarwal D, Obst J, et al. TREM2 Alzheimer's variant R47H causes similar transcriptional dysregulation to knockout, yet only subtle functional phenotypes in human iPSC-derived macrophages. *Alzheimers Res Ther.* 2020;12(1):151.
71. Yao H, Coppola K, Schweig JE, et al. Distinct signaling pathways regulate TREM2 P\phagocytic and NFkappaB antagonistic activities. *Front Cell Neurosci.* 2019;13:457.
72. Wang S, Sudan R, Peng V, et al. TREM2 drives microglia response to amyloid-beta via SYK-dependent and -independent pathways. *Cell.* 2022;185(22):4153–4169.e19.
73. Janabi N, Peudenier S, Heron B, Ng KH, Tardieu M. Establishment of human microglial cell lines after transfection of primary cultures of embryonic microglial cells with the SV40 large T antigen. *Neurosci Lett.* 1995;195(2):105–108.
74. Akhter R, Shao Y, Formica S, Khrestian M, Bekris LM. TREM2 alters the phagocytic, apoptotic and inflammatory response to Abeta(42) in HMC3 cells. *Mol Immunol.* 2021;131:171–179.
75. Jay TR, Miller CM, Cheng PJ, et al. TREM2 deficiency eliminates TREM2+ inflammatory macrophages and ameliorates pathology in Alzheimer's disease mouse models. *J Exp Med.* 2015;212(3):287–295.
76. Wolf EM, Fingleton B, Hasty AH. The therapeutic potential of TREM2 in cancer. *Front Oncol.* 2022;12:984193.
77. Zamler DB, Shingu T, Kahn LM, et al. Immune landscape of a genetically engineered murine model of glioma compared with human glioma. *JCI Insight.* 2022;7(12):e148990.

78. Genoud V, Marinari E, Nikolaev SI, et al. Responsiveness to anti-PD-1 and anti-CTLA-4 immune checkpoint blockade in SB28 and GL261 mouse glioma models. *Oncoimmunology.* 2018;7(12):e1501137.
79. Lerner EC, Woroniecka KI, D'Anniballe VM, et al. CD8(+) T cells maintain killing of MHC-I-negative tumor cells through the NKG2D-NKG2DL axis. *Nat Cancer.* 2023;4(9):1258–1272.
80. Linnartz-Gerlach B, et al. TREM2 triggers microglial density and age-related neuronal loss. *Glia* 2019;67:539–550.
81. Cantoni C, Bollman B, Licastro D, et al. TREM2 regulates microglial cell activation in response to demyelination in vivo. *Acta Neuropathol.* 2015;129(3):429–447.
82. Bungert AD, Urbantat RM, Jelgersma C, et al. Myeloid cell subpopulations compensate each other for Ccr2-deficiency in glioblastoma. *Neuropathol Appl Neurobiol.* 2023;49(1):e12863.
83. Keren-Shaul H, Spinrad A, Weiner A, et al. A unique microglia type associated with restricting development of Alzheimer's disease. *Cell.* 2017;169(7):1276–1290.e17.
84. von Roemeling CA, Wang Y, Qie Y, et al. Therapeutic modulation of phagocytosis in glioblastoma can activate both innate and adaptive antitumour immunity. *Nat Commun.* 2020;11(1):1508.
85. Feng M, Jiang W, Kim BYS, et al. Phagocytosis checkpoints as new targets for cancer immunotherapy. *Nat Rev Cancer.* 2019;19(10):568–586.